ELSEVIER

Biochimica et Biophysica Acta 1325 (1997) 1–7

BIOCHIMICA ET BIOPHYSICA ACTA
BBA

Rapid report

Characterization of the sub-main-transition in distearoylphosphatidylcholine studied by simultaneous small- and wide-angle X-ray diffraction

Karin Pressl [a], Kent Jørgensen [b], Peter Laggner [a,*]

[a] *Institute of Biophysics and X-ray Structure Research, Austrian Academy of Sciences, Steyrergasse 17 / VI, A-8010 Graz, Austria*
[b] *Department of Pharmaceutics, The Royal Danish School of Pharmacy, DK-2100 Copenhagen, Denmark*

Received 2 January 1997; revised 17 January 1997; accepted 20 January 1997

Abstract

Simultaneous small- and wide-angle X-ray diffraction was used to investigate the structural conversions in the so-called sub-main-transition of fully hydrated multilamellar vesicles of distearoyl phosphatidylcholine (DSPC). The small-angle diffraction patterns show a modification in the supramolecular structure of the corrugated lipid bilayer and reveal that the sub-main-transition does not abolish the general features of the ripple phase ($P_{\beta'}$). Concomitantly in the wide-angle region the diffraction patterns exhibit a rearrangement of the hydrocarbon chain packing and an onset of chain melting. The presence of KCl show an enhancement of the effects of the sub-main-transition. Moreover, in the ripple phase ($P_{\beta'}$) below the sub-main-transition the hydrocarbon chains are positioned on an orthorhombic lattice in the presence of KCl.

Keywords: Phosphatidylcholine; Sub-main-transition; Ripple phase; X-ray diffraction

Recently, a hitherto unknown phase transition, denoted as sub-main transition, was discovered by differential scanning calorimetry in saturated diacyl phosphatidylcholines having 17–20 carbon atoms per acyl chain [1]. The low-enthalpy phase transition is highly cooperative, extremely sharp and of first order. It is placed between the pre- and main-transition at the high-temperature end of the so-called ripple phase ($P_{\beta'}$). The ripple phase has been exhaustively studied using a variety of physico-chemical techniques, such as differential scanning calorimetry [2], X-ray diffraction [3–6], freeze-fracture electron microscopy [7,8], e.s.r. [9] and n.m.r. spectroscopy [10]. Despite of that wealth of information, accumulated over the past two decades, the physics underlying the periodic intrabilayer corrugation is still poorly understood.

In the theory of Carlson and Sethna [11], local defects (chain melting) in the void regions, which are the consequence of the packing competition between the headgroups and the chains, are held responsible for bilayer corrugation. Falkovitz et al. [12] have introduced a theory, whereby the ripple phase is

Abbreviations: DSPC, distearoyl phosphatidylcholine; SWAX, simultaneous small- and wide-angle X-ray diffraction; DSC, differential scanning calorimetry; $DC_{17}PC$, diheptadecanoic phosphatidylcholine; e.s.r., electron spin resonance; n.m.r., nuclear spin resonance

* Corresponding author. Fax: +43 316 812367. E-mail: fibrlagg@mbox.tu-graz.ac.at

0005-2736/97/$17.00
PII S0005-2736(97)00013-8

formed by a membrane endowed with spontaneous curvature that stabilizes interfaces between solid and fluid domains. A similar theory has been proposed by Marder et al. [13], who have discussed the bilayer corrugations in terms of a spatial modulation due to the existence of periodically bent microdomains composed of fluid- and solid-like domains respectively. A number of other factors have been discussed in relation to the bilayer corrugation: spontaneous local bilayer curvature arising from electrostatic coupling between water and headgroup layers [14], packing competition between relatively rigid molecules [15], and size mismatch between headgroups and chains [16], the role of intermembrane interaction [17].

So far the available data of the sub-main transition are limited to differential scanning calorimetric results for a series of saturated diacyl phospholipid bilayers of different acyl chain length [1]. In the present study, we report on the observation of the sub-main transition in distearoyl phosphatidylcholine (DSPC) by simultaneous small- and wide-angle X-ray diffraction (SWAX), and differential scanning calorimetry. We found that the sub-main transition does not abolish the general features of the ripple phase, but alters the shape of the large-scale periodic bilayer corrugations. The presence of salt (KCl) intensifies the transition. This is most pronounced in the wide-angle region, where the acyl chains in the presence of KCl are packed in an orthorhombic symmetry in the ripple phase below the sub-main transition which turns into a pseudohexagonal order above the transition.

Sample preparation. For differential scanning calorimetry, 1,2-distearoyl-sn-glycero-3-phosphocholine (DSPC) was purchased from Avanti Polar Lipids, Birmingham Alabama, and was used without further purification. The purity was checked using a Waters Millenium 2010 HPCL system (Milford, MA, USA), a 5 μm Phenomenex diol spherical column (Torrance, CA, USA), a chloroform/methanol/water (7.3:2.3:0.3, v/v) eluent and an evaporative ACS mass detector (Cheshire, UK). A single peak was observed in HPCL chromatograms confirming the purity of the lipids being far greater than 99%. Multilamellar vesicles prepared for calorimetric measurements were made by dispersion of weighted amount of dry lipids in H_2O and in 200 mM KCl, 1 mM NaN_3 solution, respectively. To ensure complete hydration, the lipid suspension was left for at least one hour at ten degrees above the main-transition temperature. During this period the lipid suspension was rigorously vortexed several times.

For X-ray diffraction, triply distilled, deionized water was used for all dispersions. Weighted amounts of dry DSPC (30% w/w) were dispersed in H_2O or in a 200 mM KCl solution, respectively, and incubated at 70°C for 3 h. The suspensions were periodically vortexed during this time. Then the samples were cycled 5–7 times between 70°C and 4°C and vortex-mixed at the higher temperature. These dispersions were hydrated for 3 h and stored for at most 48 h at 4°C. Radiation damage was checked after each measurement by using thin-layer chromatography. No trace of lysolecithin was found under the conditions of the present protocol (see below).

Diffraction scanning calorimetry. Differential scanning calorimetry was performed using a MicroCal MC-2 (Northhampton, MA, USA) power compensating calorimeter. 1.2 ml of 5-mM lipid samples were scanned in the upscan mode at 13°C/h. Before each scan the lipid suspension was equilibrated for 50 min at the starting temperature.

X-ray diffraction. Simultaneous small- and wide-angle X-ray diffraction measurements were carried out by using a modified Kratky compact camera (MBraun-Graz-Optical Systems, Graz, Austria) [18], which employs two coupled linear position sensitive detectors (PSD, MBraun, Garching, Germany) monitoring the s-ranges [$s = 2 \sin \theta/\lambda$, 2θ = scattering angle, $\lambda = 1.54$ Å] between 0.0075–0.07 $Å^{-1}$ and 0.20–0.29 $Å^{-1}$ respectively. The line-focus (Cu radiation) of a Rigaku Rotaflex Ru200 rotating anode generator (Rigaku Corp., Japan) was used, operating at 6 kW (50 kV and 60 mA). To eliminate the Cu K_β radiation, a 30 μm Ni-filter was used. The position calibration of the detectors was performed by using the diffraction patterns of Ag-stearate (small-angle region, reflection at $s = 0.0205$ $Å^{-1}$) and p-Br-benzoic acid (wide-angle region, reflections at $s_1 = 0.214$ $Å^{-1}$, $s_2 = 0.263$ $Å^{-1}$ and $s_3 = 0.270$ $Å^{-1}$) as reference materials. The samples were measured in a thin-walled 1 mm diameter Mark capillary held in a steel cuvette which provides good thermal contact to the Peltier heating unit.

Before the measurements the samples were equilibrated for about 45 min at the starting temperature.

Samples were measured at each temperature for 30 min, and the equilibration time at each new temperature setting was 5 min. Typical temperature protocols are described in the captions to Figs. 2 and 3.

Fig. 1 shows the heat curves obtained by using differential scanning calorimetry of DSPC in 200 mM KCl and in H_2O respectively. The curves exhibit the existence of a sub-main-transition positioned between the pre- and the main-transition, and demonstrate that in the presence of salt the transition enthalpy is strongly increased.

Fig. 2A,B displays the small-angle X-ray patterns of DSPC in a 200 mM KCl solution in the temperature range between 44°C and 56°C. The sub-main transition occurs at 54.3°C, and is reflected by an increase in the scattering intensity in the region around the (10) reflection and the (11) shoulder, and in a very small positional shift of the (10) reflection to higher s-values. The (11) shoulder, an indicator of the corrugation of the lipid bilayers, exists both below and above the sub-main transition, although it is more pronounced in the ripple phase below the transition.

Fig. 2C shows the corresponding diffraction patterns for DSPC in H_2O. Compared with the diffraction patterns of the system in 200 mM KCl, the curves in Fig. 2C exhibit qualitatively the same characteristics with regard to the sub-main-transition: The intensity around the (10) reflection and (11) shoulder is increased and the (10) reflection is slightly shifted to higher s-values. In the absence of salt, the (11) shoulder is more pronounced than in the KCl solution, the transition proceeds in a more continuous manner as compared to the salt solution, and the reflections throughout the whole temperature range are broader.

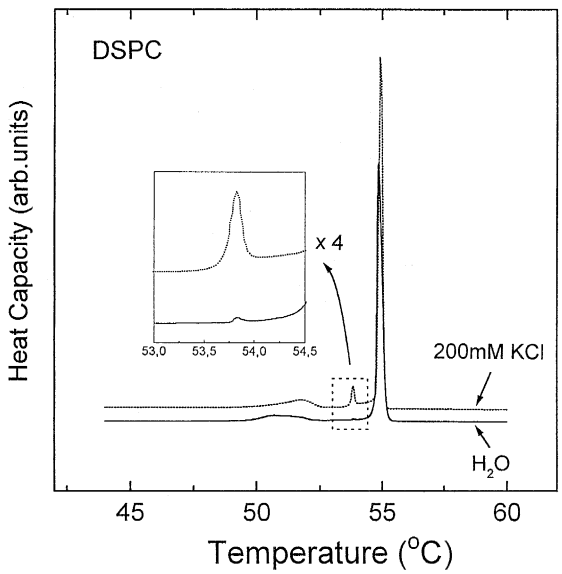

Fig. 1. Heat capacity curves obtained by DSC at a scan rate of 13°C/h for DSPC in 200 mM KCl and H_2O, respectively. The c_p-curves show the sub-main-transition positioned between the pre- and main-transition. The inset shows a magnification of the heat capacity curves in the temperature region of the sub-main-transition.

Fig. 3A,B shows the temperature scan of the wide-angle scattering patterns of DSPC in a 200 mM KCl solution ($44°C \leq T \geq 56°C$). The sub-main transition markedly diminishes the intensity of the (20) reflection of the orthorhombic subcell, slightly shifts it to smaller scattering angles and causes the shoulder at $(4.15\ Å)^{-1}$ to vanish. The continuous decrease of the intensity above the sub-main-transition points to the beginning of chain melting towards the main-transition. In the gel phase (i.c. below the pre-transition) the diffraction curves display the unequivocal pattern of an orthorhombic structure: the sharp (20) reflection is placed at $(4.25\ Å)^{-1}$, the shoulder due to the (11) reflection is placed around $(4.15\ Å)^{-1}$. The pre-transition strongly reduces the intensity of the (20) reflection but does not abolish the (11) reflection, indicative of an orthorhombic chain packing even above the pre-transition. The (20) reflection moves to a higher scattering angle and broadens as compared to the gel phase ($L_{\beta'}$), which relates to a smaller correlation length [19].

Fig. 3C displays the corresponding wide-angle diffraction patterns of DSPC in H_2O, which exhibit a clear difference to the lipid in the presence of KCl. No change in intensity of the reflection maximum is visible during the sub-main transition. Throughout the range of the ripple phase, the patterns do not show a shoulder at $(4.15\ Å)^{-1}$, which would correspond to the (11) reflection. Clearly in the gel phase ($L_{\beta'}$) the (20) reflection of the multilamellar system in H_2O is broader as compared to the lipids in KCl solution. The shoulder due to the (11) reflection in the $L_{\beta'}$-phase is not as pronounced as in the diffraction patterns of the lipids with salt.

The change in intensity of the (10) reflection and the corresponding change in the lamellar repeat distance with temperature are shown in Fig. 4A. Be-

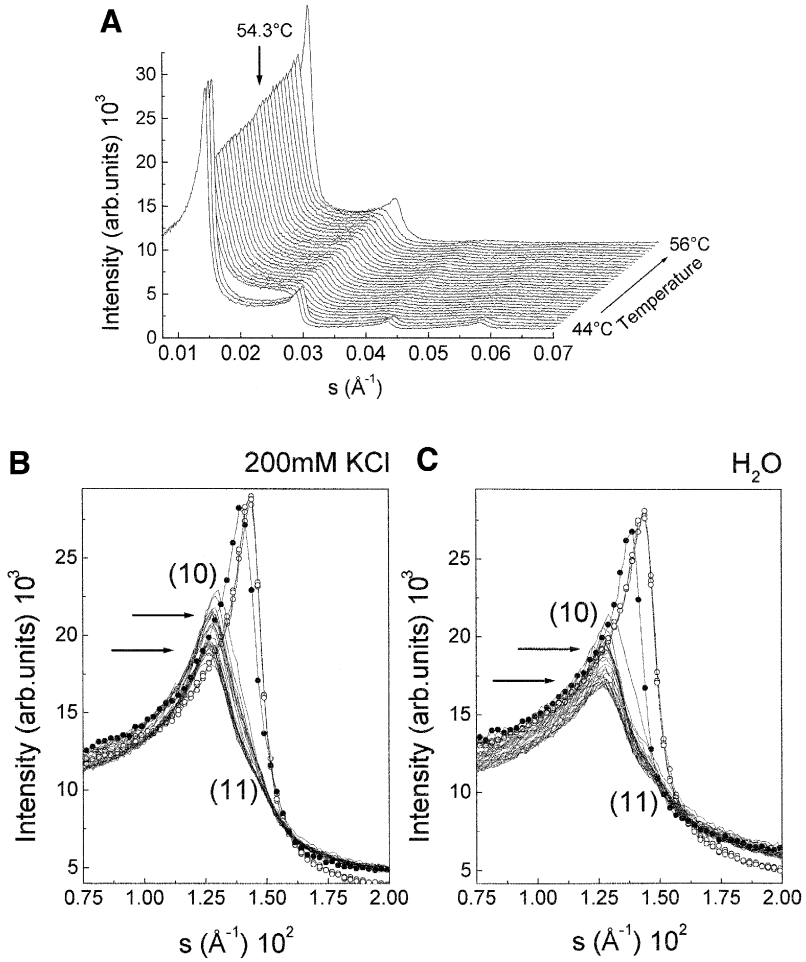

Fig. 2. A: 3D-plot of small-angle X-ray diffraction patterns of DSPC in a 200 mM KCl solution obtained upon heating in the temperature range between 44°C and 56°C. B and C: Close-up views of the first-order peak region in 200 mM KCl (B) and H_2O (C): Open circles, $L_{\beta'}$; solid lines, $P_{\beta'}$-region; closed circles, L_α. Measuring protocol: equilibration time, 5 min; measuring time, 30 min; temperature points: (44–48)°C in steps of 2°C, 51.5°C, (52.0–53.4)°C in steps of 0.2°C, (53.5–55.3)°C in steps of 0.1°C, and 56°C.

tween the pre- and the sub-main transition, the intensity slightly increases, and jumps by about 10% between 54°C and 54.6°C, and again slightly increases between the sub-main and the main-transition. Simultaneously to the intensity jump, the lamellar repeat distance decreases by less than 1 Å. This small change approaches the limits of instrumental resolution (in this region one detector channel corresponds to a change in d-spacing by 0.8 Å; $d = 1/s$), and therefore the gradual increase appears as a discontinuous jump. The lower frame in Fig. 4A shows the intensities in the (11) shoulder region. Like the intensity of the (10) reflection, it increases during the sub-main-transition by about 10%.

The intensity change with temperature of the reflection maximum in the wide-angle region and the corresponding change in its d-spacings are plotted in Fig. 4B. Between 53.7°C and 54.3°C the intensity decreases by about 5%. The intensity below and above the sub-main-transition remains constant. The d-spacings of the (20) reflection below and above the sub-main-transition respectively, differ slightly. The lower frame in Fig. 4B demonstrates that the intensity at $(4.60\ \text{Å})^{-1}$ begins to increase at 54°C.

The central task of the study was to establish the nature of structural conversions in the sub-main-transition of multilamellar vesicles of DSPC. So far this transition was only seen in differential scanning

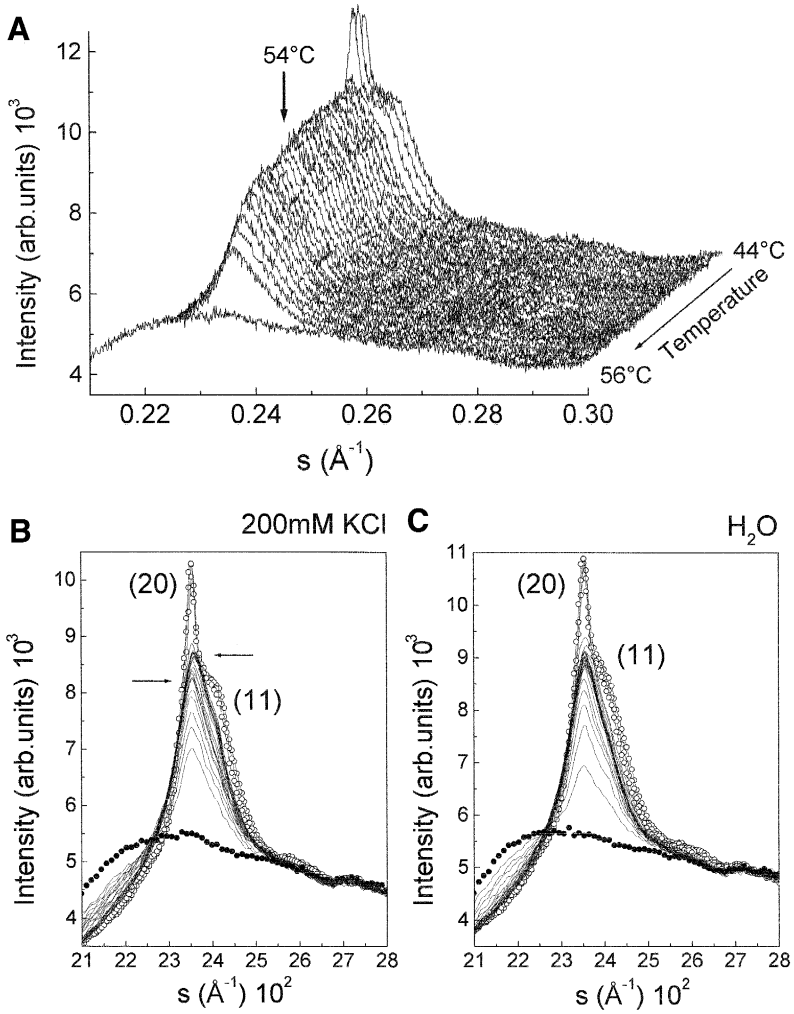

Fig. 3. (A): 3D-plot of wide-angle X-ray diffraction patterns of DSPC in a 200 mM KCl solution obtained upon heating in the temperature range between 44°C and 56°C. (B) and (C): Close-up views of the first-order peak region in 200 mM KCl (B) and H_2O (C): Open circles, $L_{\beta'}$; solid lines, $P_{\beta'}$-region; closed circles, L_{α}. Measuring protocol: equilibration time, 5 min; measuring time, 30 min; temperature points: (44–48)°C in steps of 2°C, 51.5°C, (52.0–53.4)°C in steps of 0.2°C, (53.5–55.3)°C in steps of 0.1°C, and 56°C.

calorimetric measurements [1]. Our results in the X-ray small-angle diffraction range demonstrate that the sub-main-transition modifies the supramolecular structure of the stacked corrugated lipid bilayers, but does not abolish the general features of the ripple phase. The wide-angle diffraction patterns point to a rearrangement of the hydrocarbon chain packing in the lipid matrix and a concomitant onset of chain melting during the sub-main-transition. Moreover, our wide-angle investigations show that, in the presence of KCl, the lipids exhibit an orthorhombic sub-cell packing of the hydrocarbon chains in the region between the pre- and the sub-main-transition. With regard of the effect of salt (KCl), our investigations reveal an enhancement of the characteristics of the sub-main-transition, and an enhancement of the positional packing order of the hydrocarbon chains. To facilitate the discussion, the observations in the small- and wide-angle regions are dealt with separately in the following.

Small-angle region. The presence of the (10) and the (11) reflections below and above the sub-main-transition indicates that the stacked lipid multilayer system remains corrugated. This establishes the fact

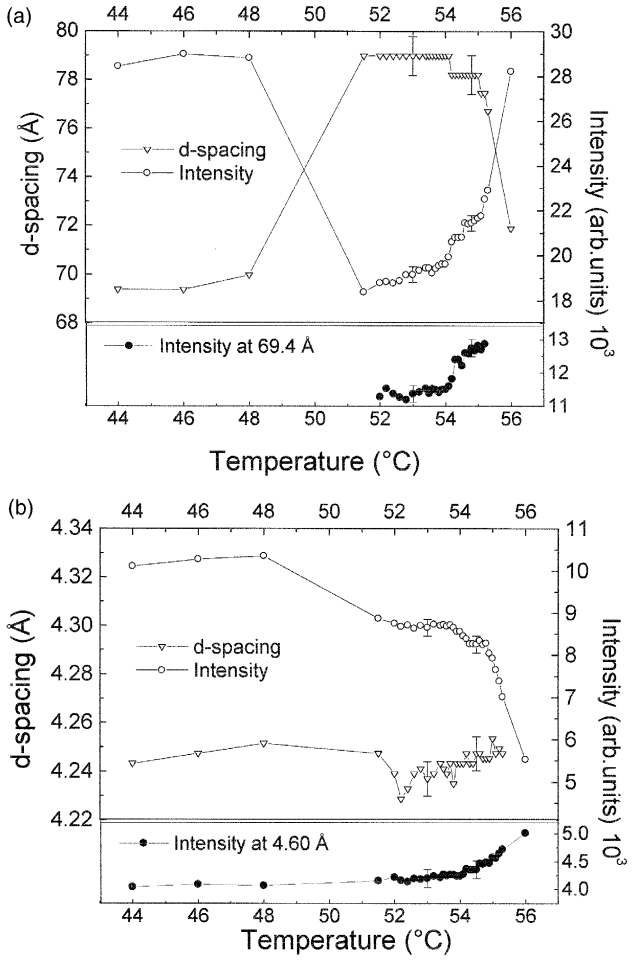

Fig. 4. Temperature dependence of the intensities of the (10) reflection and the corresponding d-spacings in the small-angle region (A) and the intensities of the reflection maxima in the wide-angle region and the corresponding d-spacings (B) of DSPC in a 200 mM KCl solution. The lower frames show the temperature dependence of the intensities at (69.4 Å)$^{-1}$ and at (4.60 Å)$^{-1}$, respectively.

that the sub-main transition occurs between two different ripple phases.

The change in the intensity of the (10) reflection and (11) shoulder, the change in the intensity ratio of the (10) and (11) reflection, and the decrease in lamellar repeat distance refers to a difference in the dimensions of bilayer corrugation in the ripple phase below and above the transition. In the following discussion we denote these two phases as ripple phase I (below the sub-main-transition) and ripple phase II (above the sub-main transition), respectively.

The intensity increase of the (10) and (11) reflections can be interpreted as an enhancement in the bilayer stacking order, including corrugations and/or modifications in size and shape of the individual domains of the facetted lipid shells [20,21].

The effect of salt on the sub-main-transition reflects itself in a different transition width. In the presence of salt, the intensity of the (10) reflection rises discontinuously while it is more gradual without KCl. The difference in the intensity ratios between the (11) and (10) reflection indicates that the corrugation of the bilayers is different in the KCl solution and in H_2O, respectively.

Wide-angle region. The increase in intensity at (4.60 Å)$^{-1}$ and the concomitant decrease of the (20) reflection intensity are indicators of the onset of chain melting. The moderate increase in the d-spacing of the (20) reflection, the decrease in the intensity of the (20) reflection, and the loss of the shoulder at (4.15 Å)$^{-1}$, all point to a rearrangement of the orthorhombic hydrocarbon chain packing below the sub-main-transition towards a pseudohexagonal symmetry above the transition.

The fact that none of the above-mentioned features are noticeable in the absence of KCl, indicates that the presence of salt strongly enhances the effect of the sub-main-transition in the hydrocarbon chain region. This agrees with the results obtained by differential scanning calorimetry, which exhibit in the presence of KCl a significant influence of ionic strength on the sub-main-transition.

The influence of KCl is also obvious in the packing of hydrocarbon chains in the lipid matrix. In the presence of salt, the appearance of the shoulder around (4.15 Å)$^{-1}$ in the ripple phase I, between the pre- and the sub-main-transition, implies that the chains are packed on an orthorhombic lattice. The shoulder is not present in the diffraction patterns of the lipids in water. We suggest that the lack of salt, and the consequent decrease in stability of hydrogen bonds in the lipid matrix, allows a positional averaging of the hydrocarbon chains from the orthorhombic packing towards a pseudohexagonal order. So far, it was generally assumed that in the ripple phase the hydrocarbon chains are packed in a hexagonal lattice [22–24].

It is important to note that there is a difference in transition temperatures as determined by the wide-

and small-angle data, respectively, which indicates that, upon heating, the modification of the corrugated suprastructure occurs at slightly higher temperature (by about half of the transition width) as compared to the rearrangement of the hydrocarbon-chains in the lipid bilayer.

Wide-angle data of diheptadecanoic phosphatidylcholine (di-C_{17}PC, i.e., by one CH_2-group shorter hydrocarbon chains than DSPC) illustrate (Pressl, unpublished results) that the appearance of the sub-main transition on the packing order of the hydrocarbon chains in the lipid matrix are not only influenced by the presence of K^+-ions, but also by the number of the carbon atoms per side chain. Similar to the case of DSPC in H_2O, the shoulder indicative of the orthorhombic chain packing is not visible in the diffraction patterns of DC_{17}PC in 200 mM KCl-solution in the ripple phase below the sub-main-transition.

It has been demonstrated that the sub-main transition is accompanied by a rearrangement and partial melting of the hydrocarbon chains. This suggests that in the ripple phases II two distinct domains coexist, in which the chains are molten, or ordered in a pseudohexagonal symmetry, respectively. The coexistence of fluid-like and gel-like domains in the ripple phase has been suggested by several previous studies [10,25].

We suggest that during the sub-main-transition chain melting proceeds close to the already existing fluid-like domains. It has been proposed by Carlson and Sethna [11] that molten chains and fully extended chains are placed in the regions of enhanced curvature in opposite halves of the sawtooth modulated bilayers. The expansion of the molten chain domains over the whole region of the steeper part of the asymmetric sawtooth modulation of the bilayer in the ripple phase II could be a possible consequence. If domains of the molten chains are responsible for the formation of the periodically rippled bilayers, which has been proposed in several theories [12,13,11], the change in domain sizes is one possible cause for the change in bilayer corrugation during the sub-main transition.

The authors wish to thank Dr. Michael Rappolt and Dr. Karl Lohner for helpful discussions. This work was supported by the Österreichischer Fonds zur Förderung der wissenschaftlichen Forschung Grant P10105-MOB (P.L.).

References

[1] Jørgensen, K. (1996) Biochim. Biophys. Acta 1240, 111–114.
[2] Lewis, R.N.A.H., Mak, N. and McElhaney, R.N. (1987) Biochemistry 26, 6118–6126.
[3] Tardieu, A., Luzzati, V. and Reman, F.C. (1973) J. Mol. Biol. 75, 711–733.
[4] Janiak, M.J., Small, D.M. and Shipley, G.G. (1979) J. Biol. Chem. 254, 6068–6078.
[5] Janiak, M.J., Small, D.M. and Shipley, G.G. (1976) Biochemistry 15, 4575–4580.
[6] Stamatoff, J., Feuer, B., Guggenheim, H.J., Tellez, G. and Yamane, T. (1982) Biophys. J. 38, 217–226.
[7] Luna, E.J. and McConnell, H.M. (1977) Biochim. Biophys. Acta 466, 381–392.
[8] Tsuchida, K., Ohki, K., Sekiya, T., Nozawa, Y. and Hatta, I. (1987) Biochim. Biophys. Acta 898, 53–58.
[9] Tsuchida, K., Hatta, I., Imaizumi, S. and Nozawa, Y. (1985) Biochim. Biophys. Acta 812, 249–254.
[10] Wittebort, R.J., Schmidt, C.F. and Griffin, R.G. (1981) Biochemistry 20, 4223–4228.
[11] Carlson, J.M. and Sethna, J.P. (1987) Phys. Rev. A 36, 3359–3374.
[12] Falkovitz, M.S., Seul, M., Frisch, H.L. and McConnell, H.M. (1982) Proc. Natl. Acad. Sci. USA 79, 3918–3921.
[13] Marder, M., Frisch, H.L., Langer, J.S. and McConnell, H.M. (1984) Proc. Natl. Acad. Sci. USA 81, 6559–6560.
[14] Doniach, S. (1979) J. Chem. Phys. 70, 4587–4596.
[15] Scott, H.L. and Pearce, P.A. (1989) Biophys. J. 55, 339–345.
[16] Sackmann, E., Rüppel, D. and Gebhardt, C. (1980) In Liquid Crystals of One and Two Dimensional Order (Helfrich, W. and Heppke G., eds.), pp. 309–326, Springer, New York.
[17] Goldstein, R.E. and Leibler, S. (1988) Phys. Rev. Lett. 61, 2213–2216.
[18] Laggner, P. and Mio, H. (1992) Nucl. Inst. Meth. Phys. Res. A 323, 86–90.
[19] Sun, W.-J., Suter, R.M., Knewtson, M.A., Worthington, C.R., Tristram-Nagle, S., Zhang, R. and Nagle, J.F. (1994) Phys. Rev. E 49, 4665–4676.
[20] Seul, M. and Andelman, D. (1995) Science 267, 476–483.
[21] Rappolt, M. and Rapp, G. (1996) Ber. Bunsenges. Phys. Chem. 100, 1153–1162.
[22] Hentschel, M.P. and Rustichelli, F. (1991) Phys. Rev. Lett. 66, 903–906.
[23] Ruocco, M.J. and Shipley, G.G. (1982) Biochim. Biophys. Acta 691, 309–320.
[24] Janiak, M.J., Small, D.M. and Shipley, G.G. (1976) Biochemistry 15, 4575–4580.
[25] Tsuchida, K. and Hatta, I. (1988) Biochim. Biophys. Acta 945, 73–80.